中國機械工程學刊第四十一卷第五期第 627~637 頁(民國一百零九年)
Journal of the Chinese Society of Mechanical Engineers, Vol.41, No.5, pp 627~637 (2020)

Construction and Application of a Stable Nodal Integration Method in Computational Electromagnetics on Tetrahedral Meshes

Hui Feng* and Xiangyang Cui**

Keywords: Stable nodal integration method, Magnetostatic, Transient eddy current, Linear tetrahedral meshes.

ABSTRACT

This paper presents a stable nodal integration method (SNIM) to solve nonlinear magnetostatic and transient eddy current electromagnetic problems. A weakened weak formulation based on nodes is firstly considered, framing the so-called node-based smoothing domains. Secondly, the integration scheme of SNIM formulation is derived by constructing appropriate equivalent smoothing domains and temporary integration points. And then, the authors use the presented method to solve various benchmark problems to observe its properties adopting linear nodal tetrahedral meshes. The results show that the proposed approach is better in sense of accuracy than traditional finite element method, and the effectiveness and potentialities of SNIM for electromagnetic applications can be witnessed.

INTRODUCTION

The usage of integrated mechatronic system has strongly increased in the design of various devices, and sensor is one of the most important elements of the mechatronic system. Precision of the sensing element is crucial to performance of the whole system. Numerical simulation for designed sensor structure is an effective way to testify its efficacy [Wu, M.T. et al., 2018; Han, R. et al., 2016; Psuj, G. et al., 2017], and it can provide instructional ameliorated orientation in preliminary design phase [Wang, J. et al., 2017; Cui, Y. et al., 2017; Yu, Y. et al., 2007]. Sensors designed based on electromagnetic principle are fairly common in practical application [Carlos, M. et al., 2015; Zhou, D. et al., 2017; Li, G. et al., 2016], so study on efficient numerical method for electromagnetic analysis is beneficial to the usage of those sensors.

Numerical algorithm for computational electromagnetics has been studied for years by researchers. Various solutions have been proposed and testified, and quite a few of these methods have been proved to be effective. Traditionally, the standard finite element method (FEM) [Bíró, O. et al., 1989] and boundary element method (BEM) [Matsuoka, F. et al., 1988] are the most widely-used numerical tools in computational electromagnetics. BEM shows advantages in solving complex and large-scale problems [Matsuoka, F. et al., 1988], since it allows the simulation of fields in unbounded domains, and FEM is commonly used to solve various problems in commercial software for its simplicity and stability. While new advanced numerical methods that suitable for complicated practical problems still capture the interest of many researchers. Meshless methods developed rapidly in recent decades, and various algorithms have been put forwarded [Belytschko, T. et al., 1994; Lai, S.J. et al., 2008; Viana, S.A. et al., 1999]. Compared with FEM, meshless methods can avoid the detailed operations for pre-processing and post-processing. But the complexity of meshless methods and the higher

Paper Receivedr November, 2018. Revised December, 2018. Accepted February, 2019. Author for Correspondence: Hui Feng

**Lecturer, School of Electromechanical and Automotive Engineering, Yantai University, Yantai 264005, PR China*

***Professor, State Key Laboratory of Advanced Design and Manufacturing for Vehicle Body, Hunan University, Changsha 410082, PR China*

computation cost hinder their development in really large-scale and complicated problems. GR Liu et al proposed a G space theory in recent years [Liu, G.R., 2010a], and it forms the foundation for a series of methods, including the node-based smoothed finite element method (NS-FEM) [Nguyen-Thoi, T. et al., 2010] and other methods. This series of methods are established in weakened-weak Galerkin forms, and adopt gradient smoothing operation to approximate the derivatives of field functions [Liu, G.R., 2010a; Liu, G.R., 2010b]. The model stiffness can be effectively softened by the smoothing operation, and a number of excellent properties can be obtained simultaneously, such as good accuracy, high convergence rate, and insensitivity to element distortion [Liu, G.R. et al., 2007]. They have been developed to solve various problems, and their applications in electromagnetics have arisen in the last years. Efforts have been made on wave propagation analysis [Soares, D., 2013] and electrostatic problems [Lima, N.Z. et al., 2012; Lima, N.Z. et al., 2014].

NS-FEM is a kind of nodal integration scheme, and it carries fairly attractive features [Liu, G.R., 2008]. In fact, nodal integration formulations have been studied for years, and their simplicity and convenience in computation captures the attention of researchers. In 1994, Belytschko et al proposed an element-free Galerkin method and used the method to analysis elasticity and heat conduction problems [Belytschko, T. et al., 1994]. The proposed method shows quite favorable features, such as high convergence rate, high precision of shape function gradients, and the convenience for post-processing and data output [Belytschko, T. et al., 1994]. However, numerical instability of the method is inherent and therefore hinders its further application [Chen, J.S. et al., 2001]. JS Chen et al proposed a strain smoothing stabilization scheme to eliminate spatial instability in nodal integration [Chen, J.S. et al., 2001, Yoo, J.W. et al., 2004]. And the papers showed that the accuracy and convergent rates of results by the stabilization conforming nodal integration method are significantly improved compared with original direct nodal integration. NS-FEM is then proposed and developed based on FEM theory [Liu, G.R., 2008]. So it captures some unique features compared with meshless solutions [Feng, H. et al., 2017]: (1) it is usually developed for tetrahedral or triangular meshes which can be easily obtained for really complicated geometries; (2) it adopts linear interpolation; (3) essential boundary conditions can be directly applied; (4) supporting domain and supporting nodes for each node are naturally formed; (5) it does not contain any parameters to be determined. Meanwhile, it acquires advantages over traditional FEMs: (1) higher convergence rate; (2) insensitivity to element distortion; (3) good accuracy; (4) its data are carried on nodes and requires no post-processing. These features make NS-FEM quite suitable for practical engineering problems. So far NS-FEM have been used in various applications, such as adaptive analysis [Nguyen-Thoi, T. et al., 2011], fracture analysis [Liu, G.R. et al., 2010c], heat transfer analysis [Wu, S.C. et al., 2009] and so on. The attractive properties of NS-FEM can be witnessed through these papers [Nguyen-Thoi, T. et al., 2011; Liu, G.R. et al., 2010c; Wu, S.C. et al., 2009]. But the application areas of NS-FEM are still limited, and the overly-soft property of nodal integration methods is considered to be the major difficulty that hinders its further development [Zhang, Z.Q. et al., 2010; Beissel, S. et al., 1996; Puso, M.A. et al., 2008]. Numerical improvements have been made to eliminate the temporal instability of NS-FEM in recent years. In [Zhang, Z.Q. et al., 2010], the authors cured the overly-soft property by adding extra stabilization terms, which inevitably incorporates uncertain parameter. Further applications of NS-FEM is still limited.

Since NS-FEM carries prominent features, a stable nodal integration method (SNIM) based on NS-FEM theory is proposed for the analysis of electromagnetic problems in this work. During our study on computational electromagnetics, it occurs to us that FEM formulations usually use quadrilateral or hexahedral elements, high order elements, and edge elements [Bíró, O. et al., 1989], and meshless methods usually adopt complex functions to approximate field variables [Lai, S.J. et al., 2008; Viana, S.A. et al., 1999]. So this work aims to achieve the utilization of linear nodal tetrahedral mesh in nonlinear electromagnetic analysis. SNIM formulation adopting linear tetrahedral mesh is developed for 3-D nonlinear magnetostatic and transient eddy current problems in this paper, and the results proved to be successful and encouraging. The authors are now working on the numerical simulation of simple structured sensors based on electromagnetic principle and the results are to

be expected.

MATHEMATICAL FORMULATION

Governing Equations

To simplify the calculation procedure, field variables in electromagnetic analysis are usually expressed into potential forms. The electromagnetic field in conductors can be derived in two basically different ways from potentials. One is to use a magnetic vector potential $\mathbf{A}$ and an electric scalar potential φ. The other is to employ an electric vector potential $\mathbf{T}$ and a magnetic scalar potential ψ. This work adopts the former one to analyze magnetostatic and transient eddy current problems.

The governing equation for magnetostatic problems in Cartesian coordinates is written as

$$V:\nabla\times\nu\nabla\times\mathbf{A}=\mathbf{J}_s \tag{1}$$

where ν is the magnetic reluctivity, $\mathbf{J}_s$ is the current density, and V denotes the whole domain in analysis.

For transient eddy current problems, the governing equations in Cartesian coordinates can be expressed as

$$\begin{aligned} V&:\nabla\times\left(\nu\nabla\times\mathbf{A}\right)+\sigma\frac{\partial\mathbf{A}}{\partial t}+\sigma\nabla\frac{\partial\varphi}{\partial t}=\mathbf{J}_s \\ V_1&:\nabla\cdot\left(-\sigma\frac{\partial\mathbf{A}}{\partial t}-\sigma\nabla\frac{\partial\varphi}{\partial t}\right)=0 \end{aligned} \tag{2}$$

where σ is the conductivity, and V_1 denotes the conducting region.

Discrete Equations by FEM

The analysis domain of 3D electromagnetic problems can be discretized by four-node tetrahedral meshes. Within each element, linear interpolation is adopted to approximate field variables. Magnetic vector potential $\mathbf{A}$ can then be expressed as

$$\hat{\mathbf{A}}=\sum_{j=1}^{n}N_j\mathbf{A}_j \tag{3}$$

where $\mathbf{A}_j$ is the field variable value at the node and N_j is the shape function of finite element method.

By using the standard Galerkin method, we can obtain the weak form of Eq. (1) as

$$\int_\Omega\mathbf{N}_i\cdot\left(\nabla\times\nu\nabla\times\mathbf{A}-\mathbf{J}_s\right)d\Omega=\mathbf{0} \tag{4}$$

Adopting the divergence theorem and applying boundary conditions, it obtains

$$\int_\Omega\nabla\times\mathbf{N}_i\cdot\left(\nu\nabla\times\mathbf{A}\right)d\Omega=\int_\Omega\mathbf{N}_i\cdot\mathbf{J}_s d\Omega \tag{5}$$

Substituting Eq. (3) into Eq. (5), the discretized system equation can be expressed in the following matrix form

$$\mathbf{KA}=\mathbf{F} \tag{6}$$

where $\mathbf{K}$ is the coefficient matrix,

$$\mathbf{K}=\begin{bmatrix}\mathbf{K}_{11} & \mathbf{K}_{12} & \cdots & \mathbf{K}_{1Node}\\ \mathbf{K}_{21} & \mathbf{K}_{22} & \cdots & \mathbf{K}_{2Node}\\ \vdots & \vdots & \vdots & \vdots\\ \mathbf{K}_{Node1} & \mathbf{K}_{Node2} & \cdots & \mathbf{K}_{NodeNode}\end{bmatrix} \tag{7}$$

$$\mathbf{K}_{ij}=\nu\mathbf{C}_{ij}=\nu\begin{bmatrix}C_{xx} & C_{xy} & C_{xz}\\ C_{yz} & C_{yy} & C_{yz}\\ C_{zx} & C_{zy} & C_{zz}\end{bmatrix}$$

$\mathbf{A}$ is the vector of node potentials,

$$\mathbf{A}=\begin{bmatrix}\mathbf{A}_1 & \cdots & \mathbf{A}_{Node}\end{bmatrix}^{\mathrm{T}},\ \mathbf{A}_i=\begin{bmatrix}A_{xi} & A_{yi} & A_{zi}\end{bmatrix}^{\mathrm{T}} \tag{8}$$

and $\mathbf{F}$ is the external current source vector.

$$\mathbf{F}=\begin{bmatrix}\mathbf{F}_1 & \cdots & \mathbf{F}_{Node}\end{bmatrix}^{\mathrm{T}},\ \mathbf{F}_i=\begin{bmatrix}F_{xi} & F_{yi} & F_{zi}\end{bmatrix}^{\mathrm{T}} \tag{9}$$

$$\begin{aligned} F_{xi}&=\int_\Omega N_i J_x dxdydz\\ F_{yi}&=\int_\Omega N_i J_y dxdydz\\ F_{zi}&=\int_\Omega N_i J_z dxdydz \end{aligned} \tag{10}$$

where $Node$ is the number of nodes in analysis, and terms of matrix $\mathbf{C}_{ij}$ can be expressed as integral equations of $\partial N_i/\partial r, \partial N_j/\partial r\left(r=x,y,z\right)$.

In the same way, the weak form of Eq. (2) can be written as

$$\begin{bmatrix}\int_V\left[\nabla\times\mathbf{N}_i\cdot\nu\nabla\times(\ )\right]dV & 0\\ 0 & 0\end{bmatrix}\cdot\begin{bmatrix}\mathbf{A}\\ \varphi\end{bmatrix}+$$

$$\begin{bmatrix}\int_V\sigma\mathbf{N}_i\cdot(\ )dV & \int_V\sigma\mathbf{N}_i\cdot\nabla(\ )dV\\ \int_{V_1}\sigma\nabla\mathbf{N}_i\cdot(\ )dV & \int_{V_1}\sigma\nabla\mathbf{N}_i\cdot\nabla(\ )dV\end{bmatrix}\begin{bmatrix}\frac{\partial\mathbf{A}}{\partial t}\\ \frac{\partial\varphi}{\partial t}\end{bmatrix} \tag{11}$$

$$=\begin{bmatrix}\int_V\mathbf{N}_i\mathbf{J}_s dV\\ 0\end{bmatrix}$$

which can also be expressed in matrix form as

$$\mathbf{M}\frac{\partial\mathbf{A}}{\partial t}+\mathbf{K}\cdot\mathbf{A}=\mathbf{F} \tag{12}$$

In non-conducting regions, coefficient matrix $\mathbf{K}$ is the same as Eq. (7), and in conducting region, extra zeros concerning φ are added in $\mathbf{K}_{ij}$ and makes it a 4×4 matrix as

$$\mathbf{K}_{ij} = \nu \mathbf{C}_{ij} = \nu \begin{bmatrix} C_{xx} & C_{xy} & C_{xz} & 0 \\ C_{yz} & C_{yy} & C_{yz} & 0 \\ C_{zx} & C_{zy} & C_{zz} & 0 \\ 0 & 0 & 0 & 0 \end{bmatrix} \quad (13)$$

$\mathbf{M}$ is a coefficient matrix concerning conductivity which exists only in conducting domain. $\mathbf{M}_{ij}$ can be expressed as

$$\mathbf{M}_{ij} = \sigma D_{ij} = \sigma \begin{bmatrix} D_{xx} & 0 & 0 & D_{x\varphi} \\ 0 & D_{yy} & 0 & D_{y\varphi} \\ 0 & 0 & D_{zz} & D_{z\varphi} \\ D_{\varphi x} & D_{\varphi y} & D_{\varphi z} & D_{\varphi\varphi} \end{bmatrix} \quad (14)$$

And $\mathbf{A}_i$ and $\mathbf{F}_i$ can be arranged correspondingly in the conducting region. All items of $\mathbf{M}$, $\mathbf{K}$, and $\mathbf{F}$ in Eq. (12) can be expressed as integral equations of $N_i, N_j, \partial N_i/\partial r, \partial N_j/\partial r$, $(r = x, y, z)$.

Node-based Smoothed Finite Element Method (NS-FEM)

To implement NS-FEM formulation, based on the tetrahedral mesh, the problem domain Ω is further divided into *Node* non-overlapping smoothing domains $\Omega_k^s (k = 1,2,\ldots,Node)$. Each smoothing domain with polyhedron shape is centered by node of the mesh. Fig. 1 shows the schematic of a typical node-based smoothing domain. Boundary of Ω_k^s is labeled as Γ_k^s and the union of all Ω_k^s forms exactly the global domain Ω.

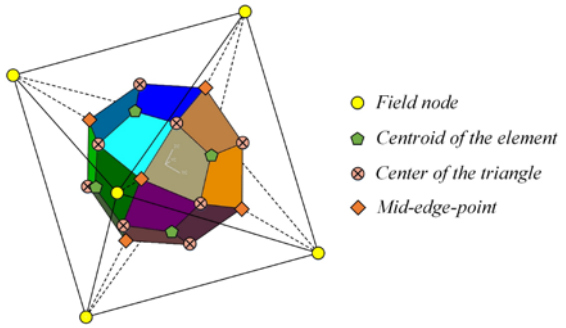

Fig. 1. Schematic of a 3D node-based smoothing domain for node k.

Adopting the node-based scheme, integration in Eq. (6) and Eq. (12) can be performed upon each smoothing domain Ω_k^s. So items $\partial N_i/\partial r, \partial N_j/\partial r (r = x, y, z)$ need to be smoothed on Ω_k^s, and the smoothing operation can be implemented upon the boundary Γ_k^s according to the divergence theorem. For example, the smoothing C_{xx} can be calculated as Eqs. (15) and (16). And other terms can be obtained in the same way.

$$\overline{C}_{xx} = \int_{\Omega_k^s} \left(\overline{\frac{\partial N_i}{\partial y}} \cdot \overline{\frac{\partial N_j}{\partial y}} + \overline{\frac{\partial N_i}{\partial z}} \cdot \overline{\frac{\partial N_j}{\partial z}} \right) d\Omega \quad (15)$$

$$\begin{aligned} \overline{\frac{\partial N_i}{\partial y}} &= \int_{\Omega_k^s} \frac{\partial N_i}{\partial y} d\Omega = \int_{\Gamma_k^s} N_i \cdot n_y d\Gamma \\ \overline{\frac{\partial N_i}{\partial z}} &= \int_{\Omega_k^s} \frac{\partial N_i}{\partial z} d\Omega = \int_{\Gamma_k^s} N_i \cdot n_z d\Gamma \end{aligned} \quad (16)$$

Stable Nodal Integration Method (SNIM)

After years of studying on numerical methods, researchers found that FEM can offer stable results for various problems. Up to now, FEM has become the most commonly used algorithm in commercial software. In contrast, NS-FEM usually provides overly-soft system [Liu, G.R, 2010a; Liu, G.R, 2010b; Wu, S.C. et al., 2009; Zhang, Z.Q. et al., 2010], and its relatively weak stability hinders its further applications [Zhang, Z.Q. et al., 2010]. To improve the stability of NS-FEM, the authors present a stable nodal integration method (SNIM) referring to the integration scheme of FEM.

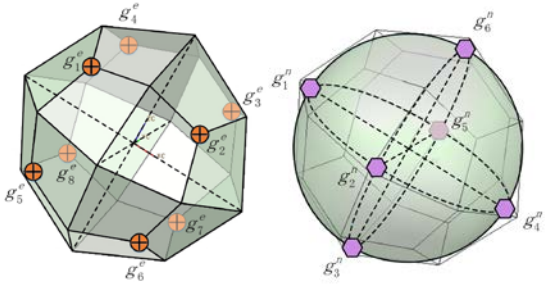

(a) (b)

Fig. 2. The integration domain and integration points for 3D problem: (a) FEM, (b) SNIM.

Fig. 2(a) shows the smoothing domain Ω_k^s and the integration points $g_i^e (i = 1,\ldots,N_e^s)$ of FEM formulation around node *k*. N_e^s is the number of surrounding elements of node *k*. To obtain the stable nodal integration scheme, Ω_k^s is approximated as a sphere domain Ω_k^{sc} with the same volume V_k^s, and then Ω_k^{sc} is subdivided into six sub-domains. The chosen integration points are $g_i^n (i = 1,2,3,4,5,6)$, which lie in *x*-axis, *y*-axis, and *z*-axis and keep the same distance l_c to node *k*, as layout in Fig. 2(b). $l_c = (3A_k^s/4\pi)^{1/3}$ is radius of domain Ω_k^{sc}.

In this way, the discrepancy between FEM and NS-FEM can be introduced into SNIM to some extent.

Name $\partial N_i/\partial r$, $\partial N_j/\partial r$ $(r=x,y,z)$ as DN . Assuming DN is continuous and derivable at the first order in Ω_k^{sc} , its Taylor expansion can be expressed as

$$DN = DN_k + \sum_{r=x,y,z}(\partial DN/\partial r)(r-r_k) \tag{17}$$

So DN at the six integration points are DN_1^{SC} , DN_2^{SC} , DN_3^{SC} , DN_4^{SC} , DN_5^{SC} , and DN_6^{SC} . And terms of smoothing matrix $\overline{\mathbf{K}}$ can be calculated upon six integration points, for instance

$$\begin{aligned}&\int_{\Omega_k^{SC}} \overline{N_{i,x}}\cdot\overline{N_{j,y}}d\Omega_k^{SC}\\ &=\sum_{m=1}^{6}\left(\left(\overline{N_{i,x}}\right)_m\cdot\left(\overline{N_{j,y}}\right)_m\right).\frac{V_k^s}{6}\end{aligned} \tag{18}$$

Considering Eq. (17), it turns out to be

$$\begin{aligned}&\int_{\Omega_k^{SC}} \overline{N_{i,x}}\cdot\overline{N_{j,y}}d\Omega_k^{SC} =\left(\overline{DNx}\cdot\overline{DNy}\right)_k\cdot V_k^s\\ &+\sum_{r=x,y,z}\Delta\overline{DNx_r}\cdot\Delta\overline{DNy_r}\cdot\frac{V_k^s}{3}\end{aligned} \tag{19}$$

where

$$\Delta\overline{DN_r}=\frac{\overline{\partial DN}}{\partial r}\cdot l_c \quad (r=x,y,z) \tag{20}$$

And $\dfrac{\overline{\partial DN}}{\partial r}$ can be calculated as

$$\frac{\overline{\partial DN}}{\partial r}=\int_{\Omega_k^s}\frac{\partial DN}{\partial r}d\Omega=\int_{\Gamma_k^s}DN\cdot n_r d\Gamma \tag{21}$$

Following the same procedure as Eqs. (18-21), all items in Eqs. (6) and (12) can be obtained by SNIM. One can observe that the derivatives of DN are smoothed on domain Ω_k^s , and are finally calculated on boundary Γ_k^s following the divergence theorem.

Finally, it is worth mentioning that the six integration points $g_i^n(i=1,2,3,4,5,6)$ are just temporary variables during our derivation process, and the integration scheme is accomplished equivalently by one point integration and stabilization terms, as shown in Eq. (19). Corresponding code can be realized conveniently by adding a couple lines concerning stabilization terms to original NS-FEM code, and the following examples testify efficacy of these terms. By the way, integration points of SNIM are the discretized nodes of original background mesh. Therefore, eddy current density or magnetic flux density values are carried on nodes and can be easily obtained or transferred. So SNIM can be considered as a kind of particle method, except that it needs background mesh in the early stage of computation.

Technique for Nonlinear Problem

The nonlinear problems are studied in following numerical examples, and the simple update with relaxation is adopted in nonlinear iteration. Since the main part of this paper lies on the node-based formulation, an easy to implement method is utilized for nonlinear treatment.

APPLICATIONS AND RESULTS

In this section, magnetostatic and transient eddy current examples of 3-D geometry are calculated using FEM and SNIM solutions to perceive efficacy of the proposed formulation. It is worth noting that $0.8\times l_c$ seems to obtain quite favorable results and is therefore utilized in magnetostatic problems.

TEAM Problem 20 (Nonlinear Magnetostatic Problem)

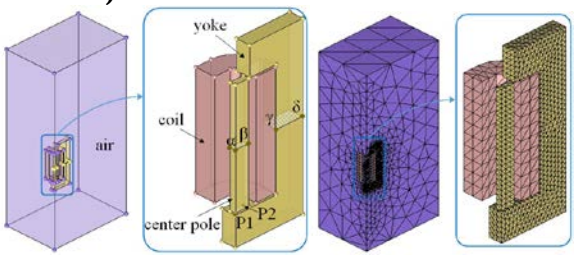

(a) (b)

Fig. 3. Geometry model and computation model of problem 20 for the TEAM Workshop: (a) a quarter geometry model, (b) computation model.

Benchmark problem 20 for the TEAM Workshop [Takahashi, N. et al., 1995] is a 3-D nonlinear magnetostatic problem. The computation model is a quarter of the original symmetry model, as shown in Fig. 3(a). The center pole and yoke are made of steel. The coil is excited by dc current. The number of turns of the coil is 381 and the ampere-turns are chosen to be 1000, 3000, 4500, 5000 in order to investigate the saturation effect [Takahashi, N. et al., 1995]. The quantities to be computed includes: (1) z-components *Bz* of flux densities at mid-point P1 $(0,0,25.75)$ and edge point P2 $(12.5,5,25.75)$ in the gap between

center pole and yoke; (2) z-components *Bz* of average flux densities along section (*α-β*) in the center pole and section (*γ-δ*) in the yoke. B-H curve of the steel is nonlinear, as demonstrated in [Takahashi, N. et al., 1995].

Results computed by FEM and SNIM are compared with experimental results. Numerical results are acquired with linear tetrahedral mesh containing 4271 nodes and 22108 elements, as shown in Fig. 3(b).

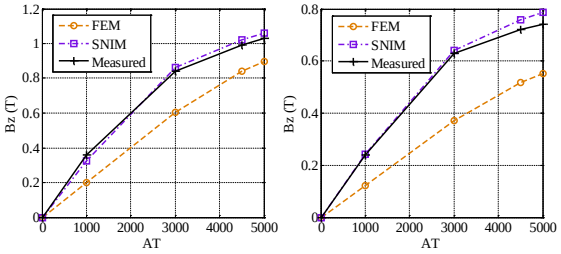

(a) (b)

Fig. 4. Z-component B_z of flux density at certain points for problem 20: (a) at point P1, (b) at point P2.

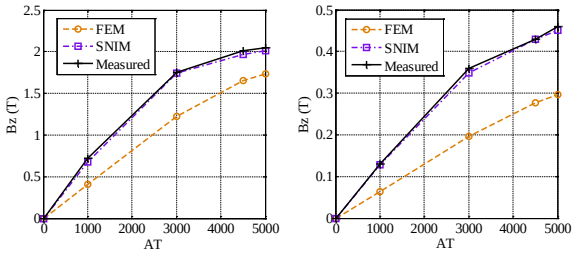

(a) (b)

Fig. 5. Z-component B_z of average flux density in certain sections for problem 20: (a) in center pole (α-β), (b) in yoke (γ-δ).

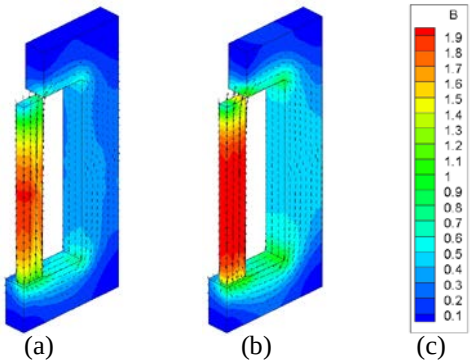

(a) (b) (c)

Fig. 6. Magnetic flux density distribution in conducting region for problem 20: (a) FEM result, (b) SNIM result, (c) legend.

Fig. 4 shows the z-directional component *Bz* of the flux density at mid-point P1 and at edge point P2 in the gap. The discrepancy of *Bz* between calculation and experiment at point P2 is larger than that at point P1, which is because the errors of computation and experiment may increase at points where the flux densities change abruptly [Takahashi, N. et al., 1995]. It is obvious that traditional FEM fails to provide results in accordance with measured data, and the maximum relative error by FEM reaches -41.01% at point P2 when adopting 3000 ampere-turn dc current. However, the proposed SNIM offers much more accurate results and reaches the maximum relative error 6.36% at point P2 when adopting 5000 ampere-turn dc current. Z-components of average flux density in the center pole (*α-β*) and yoke (*γ-δ*) are shown in Fig. 5. It is apparent that SNIM, which gets the maximum relative error -6.15% in center pole when using 1000 ampere-turn dc current, generates better approximations than FEM, whose maximum relative error reaches -50.76% in yoke when using 1000 ampere-turn dc current. And the accuracy of SNIM could be improved by finer mesh. In general, traditional FEM with linear tetrahedral mesh usually behaves relatively stiff and provides lower boundary for various fields. For electromagnetic problems with linear tetrahedral mesh, this situation becomes fairly severe. While SNIM seems to achieve quite favorable system stiffness. Fig. 6 shows the magnetic flux density results in conducting region computed by FEM and SNIM when using 5000 ampere-turns dc current. Benefits from the gradient smoothing technique, SNIM result appears to be more smooth and accurate.

TEAM Problem 13 (Nonlinear Magnetostatic Problem)

Benchmark problem 13 for the TEAM Workshop [Nakata, T. et al., 1992] is a nonlinear magnetostatic problem. The computation model that occupies one half of the whole geometry is shown in Fig. 7. An exciting coil is set between two steel channels which are not aligned with each other, and a steel plate is inserted between the channels. The B-H curve of steel is nonlinear, and the detailed expression can be seen in [Nakata, T. et al., 1992]. The coil is excited by dc current, and 1000 ampere-turn is chosen to examine the magnetic flux densities by numerical solutions. The quantities to be computed includes: (1) spatial distribution of the average flux density in the steel plates; (2) spatial distribution of absolute value of flux density along line ab.

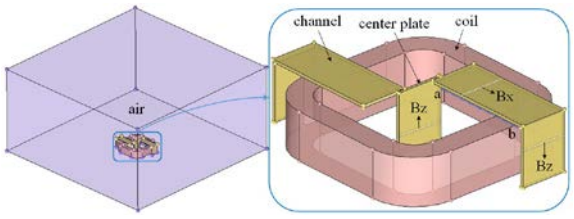

(a)

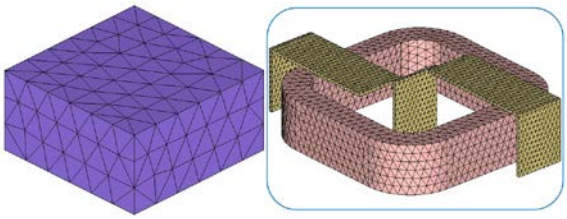

(b)

Fig. 7. Geometry model and computation model of problem 13 for the TEAM Workshop: (a) one half geometry model, (b) computation model.

Numerical results are acquired with linear tetrahedral mesh containing 14324 nodes and 80043 elements, as shown in Fig. 7. The computational and experimental magnetic flux density values in the plates and along line ab are shown in Figs. 8 and 9.

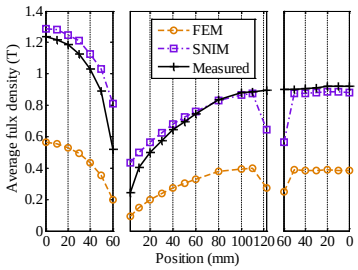

Fig. 8. Spatial distribution of average flux density in steel plates (1000AT) for problem 13.

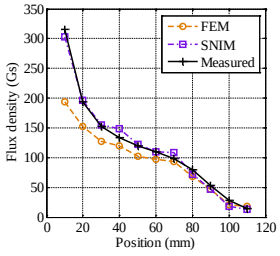

Fig. 9. Spatial distribution of absolute value of flux density in air (1000AT) for problem 13.

It is obvious that FEM solution fails to provide desirable outcomes. And since FEM results are much smaller than experimental data, the over stiff character of FEM can be observed again in this case. However, adopting the same mesh, SNIM could offer results that are generally in line with reference data except for values on corners of the plates. Therefore, effectiveness of SNIM for magnetostatic problems can be testified by above benchmark examples.

TEAM Problem 10 (Transient Eddy Current Problem)

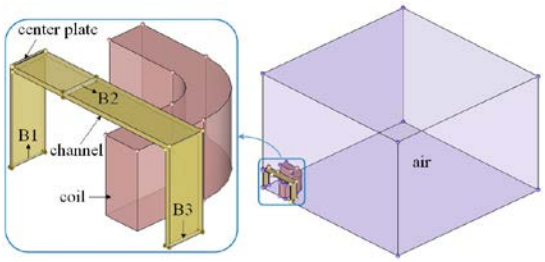

Fig. 10. Geometry model of problem 10 for the TEAM Workshop.

To illustrate the application of SNIM to transient eddy current problems, the authors programmed corresponding codes by FEM and SNIM solutions. In this subsection, these codes are used to solve benchmark problem 10 for the TEAM Workshop [Nakata, T. et al., 1995]. In this problem, an exciting coil is set between two steel channels, and a steel plate is inserted between the channels. Fig. 10 shows the geometry model, which contains one eighth of the original symmetry model for simplicity. The B-H curve of the steel is nonlinear, and is illustrated in [Nakata, T. et al., 1995]. Conductivity of the center plate and two channels is $7.505\times10^6\,S/m$. The exciting current I_0 in the coil varies with time as

$$I_0=\begin{cases}0 & (t<0)\\ I_m\left(1-e^{-t/\tau}\right) & (t\ge 0)\end{cases} \tag{22}$$

The amplitude $I_m=5.64\,\mathrm{A}$ is chosen so that the steel plates can be saturated sufficiently. Time constant $\tau=0.05s$ is selected to obtain a relatively not small and measurable eddy current density. The number of turns of the coil is 162.

In order to examine the accuracy of numerical solutions, the computed average flux densities at various positions of the steel plates (shown in Fig. 10) are compared with experimental data. In this case, to testify efficacy of mesh refinement on FEM solution, SNIM results are gained with mesh containing 8579 nodes and 45045 elements, and FEM(fine) results are gained with mesh of 23000 nodes and 126415 elements.

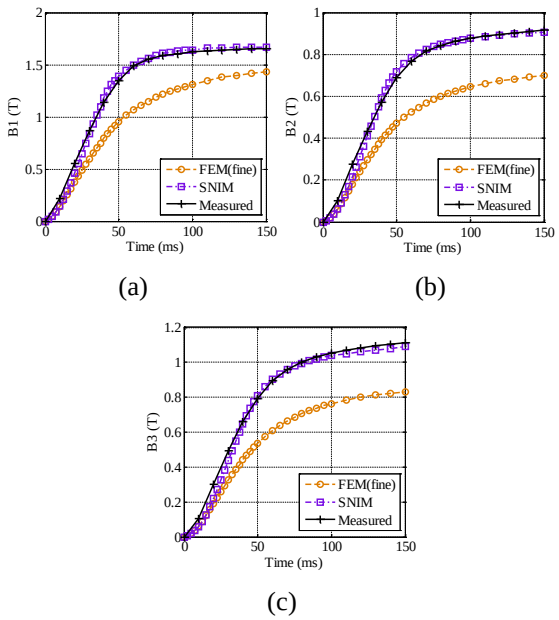

Fig. 11. Time variations of average flux density at certain sections for problem 10: (a) at position S1, (b) at position S2, (c) at position S3.

Fig. 11 shows time variation of the flux densities. It can be seen that SNIM solution acquires quite favorable results in keeping with experimental ones at various positions, and its final relative errors are 0.96%, 1.10% and 2.11%. However, large discrepancies are observed for FEM results with refined mesh, which leads to final relative errors -16.56%, -20.10% and -21.20%. Again in this case, readers could find that traditional FEM adopting linear tetrahedral mesh behaves relatively stiff and it offers much smaller results than the reference ones. While the proposed SNIM solution maintains high accuracy all along, and it seems to offer potentiality for the utilization of linear tetrahedral mesh in other complex electromagnetic problems.

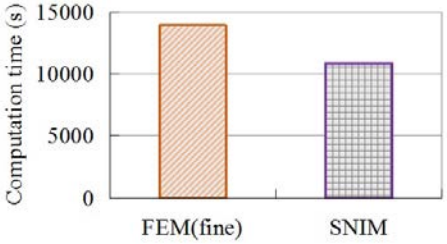

Fig. 12. Computation time of various solutions for solving TEAM Problem 10.

Except for accuracy, the computational cost analysis is also necessary to assess one new developed algorithm. To note that, results in this section were all obtained under the same platform in a computer with CPU Inter Core i5-6600 at 3.30GHz with 4.00GB of RAM memory and the Microsoft Windows 7 Professional X64 Edition V2009 operating system. All codes were written in Visual Studio 2008 Standard Edition and run with single thread. Fig. 12 shows the CPU time of the adopted solutions for solving TEAM Problem 10. It shows that the computation time of SNIM is shorter than that of FEM(fine), so the attractive feature of SNIM can be proved.

CONCLUSION

The main objective of this work is to formulate a stable nodal integration method (SNIM) with linear tetrahedral mesh for solving electromagnetic problems. It turns out that the proposed method completes well in several benchmark examples, and the magnetic flux density can be captured with high accuracy and low computation cost. And the adopted linear tetrahedral mesh is quite favorable when applied for problems with complex structure in mechatronic system. All in all, numerical examples show the adequacy of the proposed solution for electromagnetic analysis, and its attractive features produce potential for further study.

ACKNOWLEDGEMENTS

This research was funded by National Science Foundation of China, grant number 11702239. This work was also supported by the National Natural Science Foundation of China under Grant 11502227.

REFERENCES

Beissel, S., and Belytschko, T., "Nodal Integration of The Element-free Galerkin Method"; Comput. Methods Appl. Mech. Eng., Vol. 139, pp. 49-74 (1996).

Belytschko, T., Lu, Y.Y., and Gu, L., "Element-free Galerkin Methods"; Int. J. Numer. Methods Eng., Vol. 37, pp. 229-256 (1994).

Bíró, O., and Preis, K., "On The Use of The Magnetic Vector Potential in The Finite Element Analysis of Three-dimensional Eddy Currents"; IEEE Trans. Magn., Vol. 25, pp. 3145-3159 (1989).

Chen, J.S., Wu, C.T., Yoon, S., and You, Y., "A Stabilized Conforming Nodal Integration for Galerkin Mesh-free Methods"; Int. J. Numer. Methods Eng., Vol. 50, pp. 435-466 (2001).

Carlos, M., Cabrera, C., Alberto, M., Alfonso, G., and Mercedes, G., "Magnetic Sensors Based on Amorphous Ferromagnetic Materials: A Review," Sensors, Vol. 15(11), pp. 28340-28366 (2015).

Cui, Y., Yuan, H., Song, X., Zhao, L., Liu, Y., and Lin, L., "Model, Design and Testing of Field Mill Sensors for Measuring Electric Fields under High-Voltage Direct Current Power Lines," IEEE Trans. Ind. Electron., Vol. 65(1), pp. 608-615 (2017).

Feng, H., Cui, X., and Li, G., "A stable nodal integration method for static and quasi-static electromagnetic field computation," J. Comput. Physics, Vol. 336, pp. 580-594 (2017).

Han, R., Wang, T., Wang, Q., Zheng, Y., and Dong, L., "Analysis for measurement errors of DC current sensor in HVDC based on finite element method," IEEE Pes Asia-pac. Power Energy Eng. Conf., pp. 1354-1358 (2016).

Lai, S.J., Wang, B.Z., and Duan, Y., "Meshless Radial Basis Function Method for Transient Electromagnetic Computations"; IEEE Trans. Magn., Vol. 44, pp. 2288-2295 (2008).

Li, G., Wei, Z., Qian, Z., and Ma, X., "Application of ECS in metal material separation based on ANSYS," IEEE Ind. Electron. Appl., pp. 1300-1304 (2016).

Lima, N.Z., Mesquita, R.C., and Microw., J., "Point Interpolation Methods Based on Weaken-weak Formulations"; Optoelectron. Electromagn. Appl., Vol. 12, pp. 1-18 (2012).

Lima, N.Z., and Mesquita, R.C., "Face-based Gradient Smoothing Point Interpolation Method Applied to 3-D Electromagnetics"; IEEE Trans. Magn., Vol. 50, pp. 537-540 (2014).

Liu, G.R., Nguyen, T.T., Dai, K.Y., and Lam, K.Y., "Theoretical Aspects of The Smoothed Finite Element Method (SFEM)"; Int. J. Numer. Methods Eng., Vol. 71, pp. 902-930 (2007).

Liu, G.R., "A Generalized Gradient Smoothing Technique and The Smoothed Bilinear Form for Galerkin Formulation of A Wide Class of Computational Methods"; Int. J. Comput. Methods, Vol. 5, pp. 199-236 (2008).

Liu, G.R., "A G Space Theory and A Weakened Weak (W^2) Form for A Unified Formulation of Compatible and Incompatible Methods: Part I Theory"; Int. J. Numer. Methods Eng., Vol. 81, pp. 1093-1126 (2010a).

Liu, G.R., "A G Space Theory and A Weakened Weak (W^2) Form for A Unified Formulation of Compatible and Incompatible Methods: Part II Applications to Solid Mechanics Problems"; Int. J. Numer. Methods Eng., Vol. 81, pp. 1127-1156 (2010b).

Liu, G.R., Chen, L., Nguyen-Thoi, T., Zeng, K.Y., and Zhang, G.Y., "A Novel Singular Node-based Smoothed Finite Element Method (NS-FEM) for Upper Bound Solutions of Fracture Problems"; Int. J. Numer. Methods Eng., Vol. 83, pp. 1466-1497 (2010c).

Matsuoka, F., and Kameari, A., "Calculation of Three Dimensional Eddy Current by FEM-BEM Coupling Method"; IEEE Trans. Magn., Vol. 24, pp. 182-185 (1988).

Nakata, T., and Fujiwara, K., "Summary of Results for Benchmark Problem 13 (3-D Nonlinear Magnetostatic Model)"; COMPEL-Int. J. Comput. Math. Electr. Electron. Eng., Vol. 11, pp. 345-369 (1992).

Nakata, T., Takahashi, N., and Fujiwara, K., "Summary of Results for Benchmark Problem 10 (Steel Plates Around A Coil)"; COMPEL-Int. J. Comput. Math. Electr. Electron. Eng., Vol. 14, pp. 103-112 (1995).

Nguyen-Thoi, T., Vu-Do, H.C., Rabczuk, T. and Nguyen-Xuan, H., "A Node-based Smoothed Finite Element Method (NS-FEM) for Upper Bound Solution to Visco-elastoplastic Analyses of Solids Using Triangular and Tetrahedral Meshes"; Comput. Methods Appl. Mech. Eng., Vol. 199, pp. 3005-3027 (2010).

Nguyen-Thoi, T., Liu, G.R., Nguyen-Xuan, H., and Nguyen-Tran, C., "Adaptive Analysis Using The Node-based Smoothed Finite Element Method (NS-FEM)"; Int. J. Numer. Methods Biomed. Eng., Vol. 27, pp. 198-218 (2011).

Psuj, G., Biernacki, M., and Kryczyński, K., "Application of deep learning procedure to magnetic multi-sensor matrix transducer data for the need of defect characterization in steel elements," Int. Symp. Electromagn. Fields Mechatron., (2017).

Puso, M.A., Chen, J.S., Zywicz, E., and Elmer, W., "Meshfree and Finite Element Nodal Integration Methods"; Int. J. Numer. Methods Eng., Vol. 74, pp. 416-446 (2008).

Soares, D., "Time-domain Electromagnetic Wave Propagation Analysis by Edge-based

Smoothed Point Interpolation Methods"; J. Comput. Phys., Vol. 234, pp. 472-486 (2013).

Takahashi, N., Nakata, T., and Morishige, H., "Summary of Results for Problem 20 (3-D Static Force Problem)"; COMPEL-Int. J. Comput. Math. Electr. Electron. Eng., Vol. 14, pp. 57-75 (1995).

Viana, S.A., and Mesquita, R.C., "Moving Least Square Reproducing Kernel Method for Electromagnetic Field Computation"; IEEE Trans. Magn., Vol. 35, pp. 1372-1375 (1999).

Wang, J., Mu, J.Q., Ma, N., and Ma, M.L., "Simulation design of a subwavelength Fano-photonic ring resonator pressure sensor based on Finite Element Method," Opt. Int. J. Light Electron Opt., Vol. 137, pp. 195-202 (2017).

Wu, M.T., Sheng, J.P., and Bi, L.Y., "Dynamic Performance Analysis of Robot Sensor Based on Finite Element Method," Metrol. Meas. Tech., Vol. 45(2), pp. 23-27 (2018).

Wu, S.C., Liu, G.R., Zhang, H.O., Xu, X., and Li, Z.R., "A Node-based Smoothed Point Interpolation Method (NS-PIM) for Three-dimensional Heat Transfer Problems"; Int. J. Therm. Sci., Vol. 48, pp. 1367-1376 (2009).

Yoo, J.W., Moran, B., and Chen, J.S., "Stabilized Conforming Nodal Integration in The Natural-element Method"; Int. J. Numer. Methods Eng., Vol. 60, pp. 861-890 (2004).

Yu, Y., and Du, P., "Optimization of an Eddy Current Sensor Using Finite Element Method," IEEE Int. Conf. Mechatron. Automa., pp. 3795-3800 (2007).

Zhang, Z.Q., and Liu, G.R., "Temporal Stabilization of The Node-based Smoothed Finite Element Method and Solution Bound of Linear Elastostatics and Vibration Problems"; Comput. Mech., Vol. 46, pp. 229-246 (2010).

Zhou, D., Pan, M., He, Y., and Du, B., "Stress detection and measurement in ferromagnetic metals using pulse electromagnetic method with U-shaped sensor," Measurement, Vol. 105, pp. 136-145 (2017).

NOMENCLATURE

$\mathbf{A}$ magnetic vector potential
$\mathbf{A}_j$ magnetic vector potential at node j
$\mathbf{C}_{ij}$ terms that form $\mathbf{K}$ matrix by multiplying ν
$\overline{\mathbf{C}}_{ij}$ node based smoothing $\mathbf{C}_{ij}$
DN simplified expression of shape function derivatives
DN_i^{SC} DN at the integration points of SNIM
$\mathbf{F}$ the external current source vector
g_i^e integration points around node k in FEM formulation
g_i^n integration points of SNIM method
$\mathbf{J}_s$ the current density vector
k node number
$\mathbf{K}$ the coefficient matrix
$\overline{\mathbf{K}}$ the smoothing coefficient matrix
l_c distance between g_i^e and node k
$\mathbf{M}$ coefficient matrix concerning conductivity
n_r outward normal of Γ_k^s
N_e^s number of related elements around node k
N_j shape function of finite element method
V the whole geometric domain in analysis
V_1 the conducting region
V_k^s volume of Ω_k^s

Greek symbols

φ electric scalar potential
ν magnetic reluctivity
σ conductivity
Ω the whole discretized domain
Ω_k^s node-based smoothing domain
Ω_k^{sc} a sphere domain around node k with the same volume as Ω_k^s
Γ_k^s boundary of the smoothing domain Ω_k^s

一種基於四面體網格的穩定節點積分方法在計算電磁學中的構建及應用

馮慧
煙臺大學機電汽車工程學院

崔向陽
湖南大學汽車車身先進設計製造國家重點實驗室

摘要

本論文提出了一種穩定節點積分方法(SNIM)用於解決非線性靜磁和瞬態電渦流問題。首先，建立基於節點的弱-弱形式方程，同時形成基於節點的光滑積分區域。然後，構建出等效的光滑區域和輔助積分點來得到 SNIM 方法的積分方案。接下來，作者將所提出的的方法用於求解多個電磁問題的標準算例來測試其在採用線性四面體網格時的實際效果。結果表明，所提方案較傳統有限元法精度更高，並且可以看出本文方法在電磁問題中的有效性及應用潛力。